A Numerical Simulation of the Gravitational Coagulation Process for Cloud Droplets

EDWIN H. C. CHIN

Dept. of Earth and Atmospheric Sciences, Saint Louis University

AND MORRIS NEIBURGER

Dept. of Meteorology, University of California at Los Angeles

(Manuscript received 4 August 1971, in revised form 18 January 1972)

ABSTRACT

The stochastic collection process of a large drop capturing a spectrum of randomly positioned small droplets is investigated by Monte Carlo simulation, and sample growth statistics from 32 independent trials are analyzed and compared to the values obtained from integrating the growth equation. It is found that the sample mean drop mass is compatible with that predicted by the growth equation. However, the sample mean radius is significantly less than the value resulting from continuous growth at the end of 1000 sec.

The large-drop growth rate in a polydisperse cloud with an empirical spectrum is compared with that in a monodisperse cloud with the same liquid water content and the same mean volume radius. The growth rate is shown to be considerably smaller in the monodisperse cloud even though it is represented by droplets with a size that is larger than three-fourths of the droplets in the polydisperse spectrum.

The problem of cloud spectrum evolution is investigated using the kinetic equation with a set of the empirical Khrgian and Mazin spectra as initial conditions. It seems that for clouds with the same liquid water content the magnitude of R_{av} is crucial in determining the rate of the coagulation growth. Computation was also made with an initial normal distribution spectrum.

An "expected" spectrum of large droplets computed from a version of the kinetic equation for the large size end is compared with random sampling results, and substantial differences between them are found.

1. Introduction

One of the outstanding features of cloud structure is its spatial inhomogeneity. Not only do general meteorological variables such as temperature and wind fields in a cloud show nonuniformity, but measurements of direct cloud-describing characteristics such as liquid water content and droplet size distribution also display significant fluctuations. There are indications that on a scale of several hundred meters these variations may be organized (Akerman, 1967). This would be due to macroscopic meteorological processes. But fluctuations of the order of 10^{-1} to 10^{4} cm caused by turbulence are random in nature and are a significant cloud feature.

In studying single cloud-droplet growth the earlier approach was to treat the cloud as homogeneous and monodisperse. Lanmuir (1948) considered drop growth by accretion when falling through a monodisperse cloud. Bowen (1950) included condensational growth and introduced updraft but considered the cloud as represented by droplets of an "average" size. It would be of interest to see what the effect, if any, on droplet growth would be when the usual constraint of a uniform and isotropic cloud is relaxed so that the random positioning of droplets could actually be taken into account.

To study the evolution of a whole cloud spectrum, the kinetic equation for particle coagulation has been used to treat the cloud droplet collection process. Most investigators assumed an initial Gaussian distribution spectrum with respect to radius. Twomey (1966) employed a scheme of irregular spacing of radius intervals in his computations. Berry (1967) spaced data points with mass intervals in which each succeeding interval is $\sqrt{2}$ times the preceding one. Warshaw (1967) included a sedimentation term with a cloud of finite vertical extent but did not consider formation of drops $>50\,\mu$. Bartlett (1966) used a numerical scheme to simulate the collection process, but his method leads to substantial spurious mass increase if computation is carried much beyond the $40\,\mu$ limit. Kovetz and Olund (1969) included the effect of condensation. Nelson (1970) included vertical droplet transport and drop breakup effect.

It is general practice in integration of the kinetic equation that all collisions are assumed to proceed at a mean rate as prescribed by the collection kernel in a homogeneous isotropic cloud or in a cloud with only vertical inhomogeneity if a sedimentation term is included. In our investigation of the evolution of a whole cloud spectrum, this assumption is retained due to

considerations of computational economy; but an attempt is made to determine if there is any difference between the random sampling growth results and those predicted by the kinetic equation for the large-drop end of the spectrum. Both resultant spectra are reduced to dimensionless cumulative distributions to minimize effects due to differences in numerical methods before comparison.

The kinetic equation is an equation for the mean spectrum. It is also called the stochastic coalescence equation. But in the treatment of its integration, no randomness has generally been introduced either through the initial conditions or through the collision rate kernal. In the formulation of the collision kernel, the probability of collision between droplets of different sizes has been invoked. But once this is done, the collection process is allowed to proceed according to this mean rate. Specifically, when the collisions between droplets of size i and j in a unit volume in time Δt are determined by one set of $n_i n_j$, given initially or as a result of computation at any subsequent time, and with collision efficiency and relative velocity as known functions of sizes i, j, no fluctuation of this process is possible. The whole problem of spectrum evolution thus becomes an initial-value problem and the initial conditions uniquely determine the cloud spectrum at any later time. This spectrum, however, should be interpreted as an "expected" one. As an illustration of the likelihood of deviation from this expected spectrum, we shall consider a specific typical cloud. In a well-mixed cloud with liquid water content 1 gm m^{-3} and droplet concentration 10^3 cm^{-3}, the droplet mean volume radius is equal to 6.5 μ while the mean spacing between droplet centers is approximately 10^3 μ. The probability of one large droplet collecting two or more droplets at the same time is negligible if Δt is chosen to be sufficiently small that the events of droplet collection can be considered as independent. Suppose the concentrations of the droplets are $N, n_1, n_2, \cdots, n_m$, where $N=N(r_i)\Delta r$ is the concentration of large drops and $n_j=n(r_j)\Delta r$ the number of the j-sized droplets per unit volume with $r_i > r_m$. The probability that in N trials x_0 of the large drops will not collect any small droplet, that x_1 of the N drops will collect droplets of size 1, that x_2 will collect droplets of size 2, etc., in time Δt will be given by the multinomial law

$$p(x_0,x_1,x_2,\cdots,x_m) = \binom{N}{x_0,x_1,x_2,\cdots,x_{m-1}} P_{i0}^{x_0} P_{i1}^{x_1} P_{i2}^{x_2} \cdots P_{im}^{x_m},$$

where

$$\sum_{j=0}^{m} x_j = N, \quad \sum_{j=0}^{m} P_{ij} = 1, \quad P_{i0} = 1 - \sum_{j=1}^{m} p_{ij},$$

P_{ij} being defined by Eq. (2). The first and second moments are

$$\mu_j = NP_{ij}, \quad j=0, 1, 2, \cdots, m$$

$$\sigma_{jk} = \begin{cases} -NP_{ij}P_{ik}, & j \neq k \\ NP_{ij}(1-P_{ij}), & j=k \end{cases}$$

where

$$\sigma_{jk} \equiv E[(x_j-\mu_j)(x_k-\mu_k)].$$

These expressions are valid for the time step under consideration; for the next time step all the P's will have undergone changes. It is, therefore, difficult to arrive at expressions which yield information about the relative deviations and confidence intervals for a whole spectrum at an arbitrary time t. This is one of the reasons that leads us to undertake this random sampling study of a relatively idealized process.

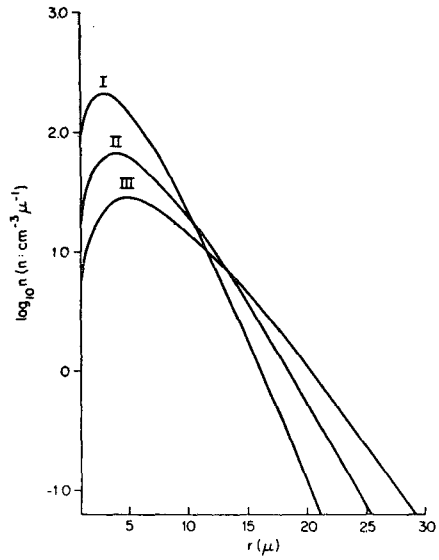

FIG. 1. Khrgian and Mazin spectra with $L=1$ gm m^{-3} for $R_{av}=4.5\,\mu$ (I), $R_{av}=6.0\,\mu$ (II), and $R_{av}=7.5\,\mu$ (III).

2. Random sampling of large-drop growth in a polydisperse cloud and comparison with results predicted by the growth equation

The empirical Khrgian and Mazin spectrum (hereafter referred to as K-M) of the form

$$n(r) = Ar^2 e^{-Br} \tag{1}$$

is used to represent the cloud droplet spectrum (Fig. 1). It is characterized by two parameters, the liquid water content L and the average radius R_{av}. In cgs units $A=(1.45/R_{av}^6)L$ and $B=3/R_{av}$. In all computations, a spectrum radius class interval of 2 μ was used, with the class being characterized by its middle value. The spectrum was truncated at the size where the concentration became less than 10^{-1} cm^{-3}, and the concentration in every size class was then multiplied by a factor

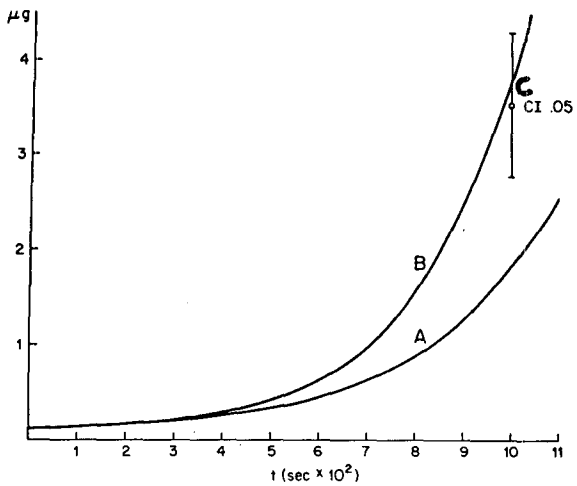

FIG. 2. Comparison of mass growth, $R_0=30\,\mu$, $L=1$ gm m^{-3}: in a monodisperse cloud, $R_v=10\,\mu$ (A); in a cloud with a K-M spectrum, $R_v=10\,\mu$ (B); and the mean mass from random sampling, for cloud B, $n=32$, showing the 95% confidence interval at $t=1000$ sec (C).

very slightly greater than 1 to make the liquid water content exactly the prescribed value. The smallest class mark to be taken into account was always $3\,\mu$.

Computations were made simulating the growth of a large droplet with initial radius $30\,\mu$, falling through a cloud with a drop size distribution represented by curve III in Fig. 1, i.e., by a K-M spectrum with $R_{av}=7.5\,\mu$ and $L=1$ gm m^{-3} and a droplet size range from 3 to $29\,\mu$. The cloud spectrum was assumed to be time-independent, i.e., the small effect on the spectrum due to collisions is neglected. Because the droplets are randomly positioned, the large-droplet growth process is probabilistic in nature.

The probability of a large drop of radius R_i collecting one smaller droplet of radius r_i due to hydrodynamic capture in a time step Δt is

$$P_{i\,i+j}\equiv P_{ij}=\pi R_i^2 Y_c^2(U_i-U_j)n_j\Delta t, \qquad (2)$$

where:

- R_i radius of large droplet
- Y_c linear collision efficiency between droplets of size i and j, the values used being those of Shafrir and Neiburger (1963) as approximated by Berry (1967)
- U_i terminal velocity of large droplet
- U_j terminal velocity of small droplet
- n_j $n_j\equiv n(r_j)\Delta r$, the number of droplets with radius between $r_j\pm 1/2\Delta r$ per unit cloud volume

Hereafter, the concise notation P_{ij} will be adopted in place of $P_{i\,i+j}$, which is the one-step transitional probability for the collector droplet from size i to $i+j$. The time step Δt is chosen in such a way that P_{ij} satisfies the consistency requirement for probability mass function, i.e.,

$$P_{ij}\geqslant 0,\quad \sum_{j=0}^{m} P_{ij}=1,$$

where

$$P_{i0}=1-\sum_{j=1}^{m} P_{ij}\geqslant 0.$$

Here P_{i0} is the probability of no collision and the mth class represents the largest size in the spectrum.

A random number x uniformly distributed over the interval (0,1) is generated at each time step by a multiplicative congruential method. The magnitude of this random number is then compared with all possible

$$\sum_j P_{ij}'s,\quad j=0, 1, 2, \cdots m.$$

If

$$\sum_{j=0}^{k-1} P_{ij}<X\leqslant \sum_{j=0}^{k} P_{ij},$$

a collision with a small droplet size k is simulated and the mass of the large droplet grows by a discrete increment due to accretion. Then the radius of the large drop, its terminal velocity, linear collision efficiencies with all the different small droplets, and finally P_{ij}, $j=0, 1, 2\cdots m$, are all recalculated with this new mass and another random number is generated to start a new cycle. A variable time step is employed in this simulation. As the drop grows in size, the length of the time step is correspondingly reduced to keep the consistency condition always intact and the magnitude of $U_i\Delta t$ the order of 10 cm. If no collision has occurred in a time step, the time count is advanced and the cycle repeats again. In essence, as the large droplet falls through the cloud with droplets randomly positioned in space, its growth history is constructed.

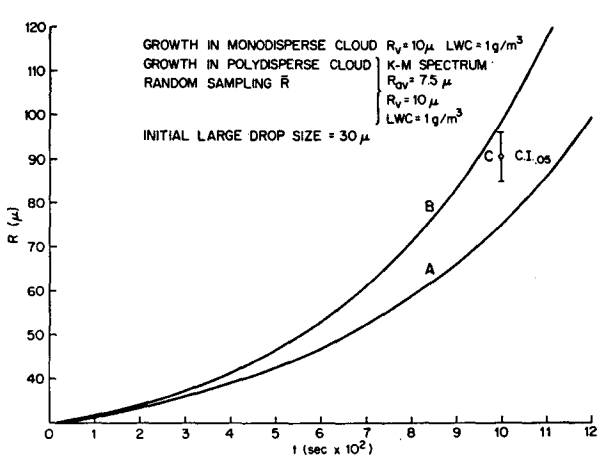

FIG. 3. Comparison of radius growth for $R_0=30\,\mu$, $L=1$ gm m^{-3}: in a monodisperse cloud, $R_v=10$ (A); in a cloud with a K-M spectrum, $R_v=10$ (B); and the mean radius from random sampling, for cloud B, $n=32$, showing the 95% confidence interval at $t=1000$ sec (C).

A total of 32 independent trial simulations of the growth of drops initially 30 μ in radius falling through the specified K-M III cloud were carried out. In this way it was possible to trace the growth histories of 32 randomly chosen 30 μ drops. The average mass and radius and the 95% confidence intervals at the end of 1000 sec of growth are shown at point C in Figs. 2 and 3.

The continuous growth equation, in which the cloud is treated as though the liquid content were uniformly distributed through space, is usually written for a monodisperse cloud as

$$\frac{dR}{dt}=\frac{N\pi r^3}{3}Y_c^2(U_R-U_r). \tag{3a}$$

This can be generalized to allow for the effect of variation of droplet size on collision efficiency, i.e.,

$$\frac{dR}{dt}=\frac{\pi}{3}\int_0^R n(r)r^3Y_c^2(U_R-U_r)dr. \tag{3b}$$

To get some indication of the separate effects of the size and special distributions of the cloud droplets on the growth of the large drop, Eq. (3b) was integrated with the same K-M III cloud spectrum as was used in the random experiment, and (3a) was integrated for a monodisperse cloud with droplet radius 10 μ equal to the mean volume radius of K-M III and with the same liquid content of 1 gm m^{-3}. In Figs. 2 and 3, curve A gives the growth in the monodisperse case, and curve B that for the polydisperse cloud.

Comparison of curves A and B show that even though about 75% of the droplets are less than 10 μ in the K-M III spectrum, droplets $>10\,\mu$ made such a major contribution that the assumption that the cloud could be approximated by a monodisperse cloud of 10 μ radius drops would result in a gross underestimation of the large-drop growth rate.

The relation between point C and curve B gives some

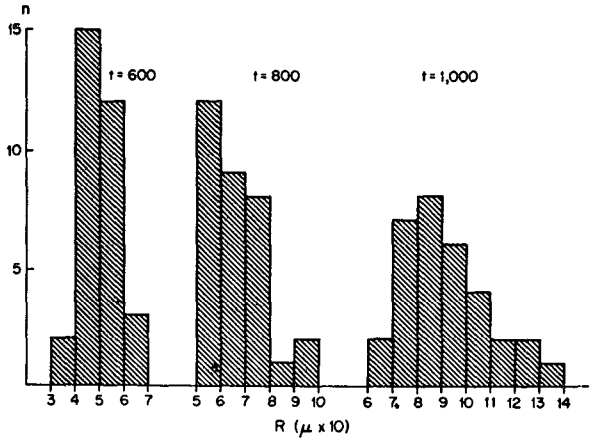

FIG. 4a. Random sampling distribution of drop sizes for $t=600$, 800 and 1000 sec, $R_0=30\,\mu$, $n=32$.

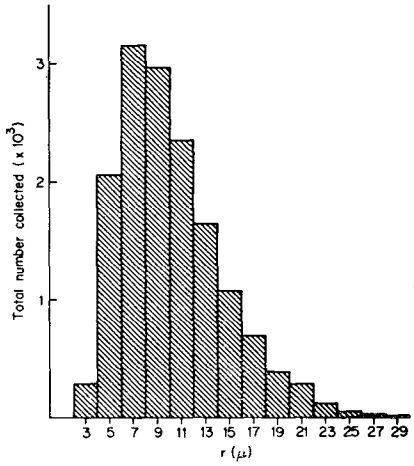

FIG. 4b. Size distribution of cloud droplets collected in 1000 sec by 32 drops with $R_0=30\,\mu$.

indication of the influence of random positioning of the droplets on the growth. To see whether the differences between C and B are significant, the 95% confidence intervals for the sample growth statistics with droplets randomly positioned are shown by vertical lines. Because the growth simulations were conducted as independent trials, the resultant radii (masses) X_i, $i=1, 2, \cdots 32$, constitute a sequence of independent identically distributed random variables. Furthermore, σ_x^2 is bounded due to the physical constraint of conservation of water mass. Therefore, it is justified to claim that this sequence has the central limit property and to construct confidence intervals accordingly. Figs. 2 and 3 show that for drop mass at 1000 sec, the value 3.85 on curve B falls within the 95% confidence interval for the mean mass, and that there is no significant difference between the sample mean mass and the value obtained from the continuous growth equation. For drop radius, however, the 95% confidence interval does not contain the continuous growth value. Since Student's t test statistic, with a value of 2.18, also falls into the critical region with a significance level of 0.05 and 31 degrees of freedom, this indicates that the sample mean radius is significantly smaller than would result from uniform growth. Growth in a non-uniform cloud with droplets randomly positioned in space resulted in a distribution in size for these n large drops with a mean radius smaller than that for the uniform case. The implication is that the basic observed cloud feature of droplets randomly located in space, in contrast with a "homogeneous" cloud, does contribute to spectrum broadening even though the liquid water content in this study is locally smooth to a scale of 10 cm.

The average time required for the "most fortunate" one-eighth of the large drops in the sample to reach a size of 100 μ is 877 sec compared with $\sim$1020 sec required by continuous growth. It could be inferred that under the same conditions—steady state K-M spectrum III, 100% relative humidity and no large-

drop interaction—if there are initially 80 drops of 30 μ size per liter, then after 15 min about 10 of these would reach 100 μ size. The coefficient of relative dispersion for the sample parameters also show a tendency to increase with time. Histograms of the size distribution from the random sample are shown in Fig. 4a for three different times, while the distribution of collected small droplets is shown in Fig. 4b.

3. Simulation of cloud spectrum evolution

The evolution of a warm cloud begins with nucleation and growth of small droplets by vapor diffusion. Once a cloud is formed and the larger drops reach adequate size, collision and coalescence between droplets of different sizes due to their relative velocities in the gravitational field become important. Conceptually, the complete kinetic equation for the changes in the droplet size distribution in an elementary cloud volume has the form

$$\partial n(v)/\partial t = -\nabla_H \cdot (\mathbf{V}n) - \partial[(V_z - U)n]/\partial z - \nabla \cdot (D\nabla n) - \left[\partial\left(\frac{dv}{dt}n\right)\Big/\partial v\right] + \frac{1}{2}\int_0^v n(u)n(v-u)K(u, v-u)du - n(v)\int_0^\infty n(u)K(u,v)du + \Phi(v), \quad (4)$$

where:

- $n(v)$ number density of droplets of size v, at time t and at a position in space with positive vector r; $n(v)dv$ thus represents the number of droplets in the size range v to $v+dv$ per unit volume and could properly be written as $n=n(v,t,r)$.
- $\mathbf{V}$ wind velocity vector
- V_z updraft speed
- U downward speed of fall of droplets of size v
- D coefficient of eddy diffusion on the scale of the cloud drop size
- dv/dt volume change due to condensation or evaporation
- $K(u,v)$ collection rate kernel denoting the rate of binary combinations between u and v size droplets due to physical processes which may include: (i) Brownian coagulation for very small droplets; (ii) collection due to relative movement caused by electric charges carried by droplets and/or by the existence of an electric field in the elementary volume; (iii) hydrodynamic capture due to relative velocities between droplets of different sizes in the gravity field modified by the forces generated by the motions of droplets in a viscous medium; and (iv) collection caused by turbulence
- $\Phi(v)$ a function characterizing the nucleation of new droplets, the breakup of large drops, and all other possible processes which may cause the generation or destruction of v size droplets.

Eq. (4), with a perfectly general collection kernel that includes all possible processes, together with the equation of condensational growth, the appropriate equations of motion, the heat balance equation for cloud droplets, the equation of state, etc., (Koo, 1962) and the proper initial and boundary conditions including the nuclei spectrum, constitutes a complete system. In theory, the distribution of cloud droplets and precipitation particles in every elementary volume from the cloud's inception up to the time of dissipation, either due to "rain-out" or evaporation, can be predicted. Aside from the formidable mathematical difficulties in solving this set of equations and the uncertainties in specifying some of the initial and boundary conditions as well as the eddy diffusion coefficient D, this approach to the problem of spectrum changes aims at predictions that are over-detailed. If one is interested in studying the behavior of spectrum evolution in general, the following assumptions are usually made:

1) An unbounded, homogeneous and isotropic cloud with a given initial spectrum (presumably produced by condensation) in a size range where Brownian coagulation is unimportant.

2) Still air, with no ambient electric field within the cloud and the droplets uncharged.

3) A relative humidity of 100% in the cloud, or more correctly, an idealized ambient vapor density field at equilibrium with each droplet regardless of its size, with no vapor transfer and no phase change being allowed.

4) $\Phi(v)=0$.

With these assumptions, Eq. (4) reduces to the familiar form

$$\partial n(v)/\partial t = \frac{1}{2}\int_0^v n(u)n(v-u)K(u, v-u)du - n(v)\int_0^\infty n(u)K(u,v)du. \quad (5)$$

Unlike Eq. (4), (5) is complete by itself and applies to the aforementioned model cloud which grows by gravitational collection and does not exchange mass with the environment. Here $n(v)=n(v,t)$ is no longer a function of position, but is a distribution representative of the cloud as a whole. This is the basic kinetic equation that has been used by several investigators to study the warm rain process.

Because (5) is a nonlinear integro-differential equation, analytic solutions can be obtained only under very restrictive assumptions of the initial distribution func-

tion and the collection rate kernel. In this section, the spectrum evolution was arrived at through simulation of (5). The first term on the right-hand side represents the gain in the number of size v droplets as a result of collisions between droplets of size u and $v-u$; the second term takes into account the loss of size v droplets by collisions of v size droplets with droplets of all other sizes. In the following computations the simulated size range extends from 3 to 201 μ with data points spaced at radius intervals of 2 μ.

The collection rate kernel for hydrodynamic capture between droplets of size i and j $(i>j)$, designated as K_{ij}, is $\pi R_i^2 Y_c^2(U_i-U_j)$. Then the expected number of droplets of size i collecting droplets of size j in a unit cloud volume in time Δt becomes

$$\Delta n_{ij}=K_{ij}n_i n_j \Delta t.$$

Here for $R_i<19\,\mu$, the value of Y_c used was that given by Davis and Sartor (1967); otherwise, Y_c was the same as mentioned previously.

In general the large drops produced as a result of coalescence between droplets of size i and j will not have mass distribution boundaries coinciding exactly with those of a size class in the spectrum; the mass will thus be distributed into two size classes. We define m_i^- and m_i^+ to be the lower and upper mass boundaries, respectively, for the size class i and m_i to be the mass corresponding to the central radius of class i. For every size combination i, j one can locate a new size class k such that $m_k^-<(m_i^+ + m_j^+)<m_k^+$. Then the number of the large drop formed will be distributed into classes k and $k-1$ according to the factors g_{ij} and f_{ij}, respectively, where

$$\left.\begin{aligned} g_{ij}&=[(m_i^+ + m_j^+ - m_k^-)(m_i+m_j)]/\\ &\qquad [(m_i^+ - m_i^- + m_j^+ - m_j^-)m_k]\\ f_{ij}&=(m_i+m_j-g_{ij}m_k)/m_{k-1} \end{aligned}\right\}. \quad (6)$$

The changes in droplet concentration in every size class are computed by the following numerical scheme where superscripts denote time step sequence:

$$\left.\begin{aligned} n_i^{t+\frac{1}{2}}&=n_i^t-\tfrac{1}{2}\sum_j \Delta n_{ij}{}^t+\tfrac{1}{2}\sum_c\sum_d f_{cd}\Delta n_{cd}{}^t\\ &\qquad +\tfrac{1}{2}\sum_p\sum_q g_{pq}\Delta n_{pq}{}^t\\ \Delta n_{ij}{}^{t+\frac{1}{2}}&=K_{ij}n_i{}^{t+\frac{1}{2}}n_j{}^{t+\frac{1}{2}}\Delta t\\ n_i^{t+1}&=n_i^t-\sum_j \Delta n_{ij}{}^{t+\frac{1}{2}}+\sum_c\sum_d f_{cd}\Delta n_{cd}{}^{t+\frac{1}{2}}\\ &\qquad +\sum_p\sum_q g_{pq}\Delta n_{pq}{}^{t+\frac{1}{2}} \end{aligned}\right\}, \quad (7)$$

where:

$t=0, 1, 2, \cdots$
$i=1, 2, 3, \cdots$
$j=1, 2, 3, \cdots$
c,d: all c,d with $m_i^-<(m_c^- + m_d^-)<m_i^+$ and $c>d$
p,q: all p,q with $m_i^-<(m_p^+ + m_q^+)<m_i^+$ and $p>q$

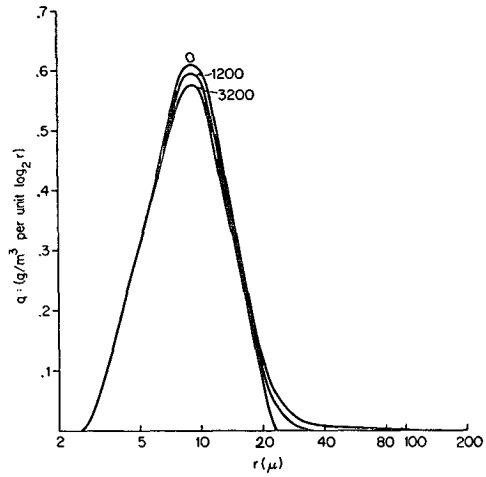

FIG. 5. Evolution of spectrum I due to collection.

Since water mass is conserved at each time step by this method, it is conserved for all time except for errors due to round-off; results for any complete computation in which such errors reached 1% were rejected.

If any of the computed concentrations for a newly formed droplet was less than 10^{-12} or, equivalently, the probability of its formation in a time step was less than one for a volume of a million cubic meters of cloud air, this event was considered as meteorologically insignificant, and not allowed to "happen." The computation process was then retracted and the original number densities were restored to the droplet classes which would have combined to produce that new class. In this manner, water mass integrity is maintained. The time step used in calculation was 2 sec. Computations were also carried out for one case with the time step halved but there was no significant difference in the results.

The changes in cloud spectrum due to collection can be best displayed in terms of water mass transfer to the

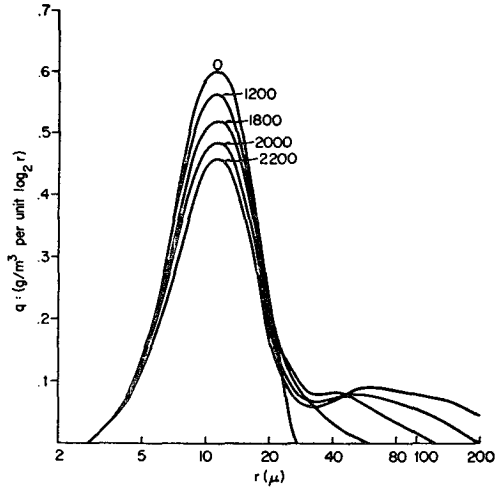

FIG. 6. Evolution of spectrum II due to collection.

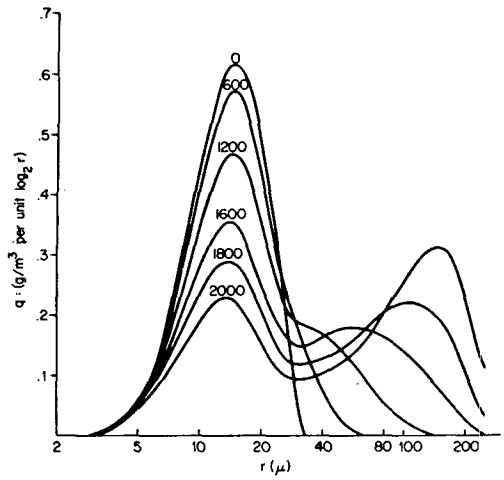

FIG. 7. Evolution of spectrum III due to collection.

larger size end. For this purpose, a graph of specific water content q grams per cubic meter per unit of $\log_2 r$ vs radius r is appropriate. When the radius is plotted on a logarithmic scale then the area under the curve between any two ordinates represents the liquid water contained by droplets with radii between these values in one cubic meter of cloud. The total area under the curve represents the liquid content of the whole spectrum and should remain constant since mass is conserved in a pure collection process. Figs. 5–7 show the changes in the three K-M spectra shown in Fig. 1 due to collection. In the case of spectrum I (Fig. 5), the transfer of mass toward the leading edge was rather slow; after 3200 sec only 0.2% of the mass had moved beyond 100 μ. For spectrum II, with $R_{av}=6\,\mu$, the rate increased notably and a second mass maximum appeared at 1800 sec at about 40 μ and moved toward the right with gradually increasing amplitude with time. For the case of spectrum III, with an initial R_{av} of 7.5 μ, the ridge appeared shortly after 1200 sec; thereafter, mass was rapidly transferred from the small droplets to the larger size end as evidenced by the rightward propagation and increasing amplitude for the new ridge and the decrease in amplitude of the original maximum. By 1800 sec, precipitation should have been initiated due to the large number of drops $>100\,\mu$ radius.

The corresponding changes in droplet numbers due to the collection process are shown in Fig. 8 in which the ordinates represent specific concentration per cubic centimeter per unit $\log_2 r$. Different scales are used in order to permit comparison of the three spectra. It is seen the reduction in the area under the curves that for all three spectra the total number of droplets decreased with time, with the annihilation of many small droplets being compensated for by a very limited increase in number in the larger sizes; i.e., the formation of large drops at very low concentration took up the mass contributed by many smaller droplets.

The growth of the 100th largest drop in a cubic meter

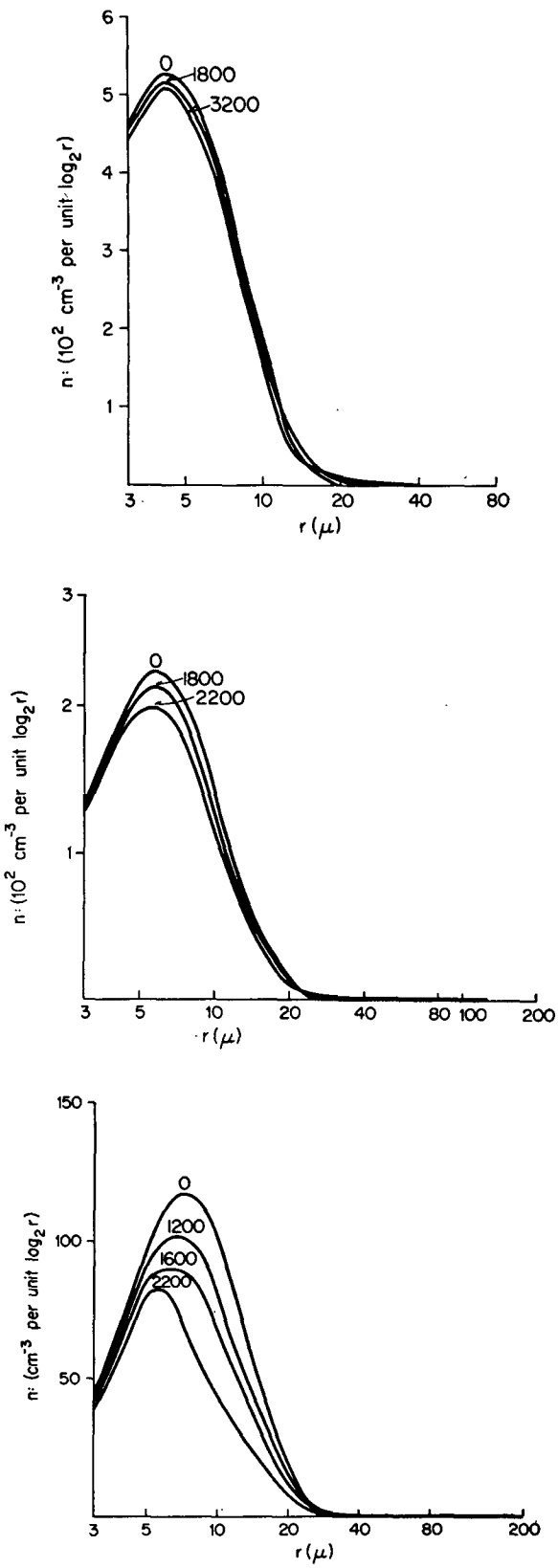

FIG. 8. Changes in droplet concentration for spectrum I, a., spectrum II, b., and spectrum III, c.

of cloud is shown in Fig. 9a. At 20 min the 100th largest drops were 39, 77 and 125 μ for K-M spectra I, II and III, respectively, while at 30 min they were 53, 141 and 187 μ. It took spectrum I, for which the initial R_{av} was 4.5 μ, 47 min to have the 100th largest drop per cubic meter to reach a size of 100 μ, while only 17 min were required for spectrum III. Fig. 9b shows the growth in mean volume radii R_v, where the growth rates are proportional to the slopes of the curves. Since all three spectra have the same liquid water content of 1 gm m^{-3} and only differ in the parameter R_{av}, it seems that the initial average radius exerts a predominant control on the subsequent growth of a spectrum.

Computations were also carried out for other cases. Fig. 10 shows the spectrum evolution for an initial K-M spectrum for which R_{av} was 4.5 μ and the liquid water content 0.3 gm m^{-3}, cloud characteristics corresponding to a mid-latitude thick stratus. Changes in the curve of specific water content q vs radius are barely noticeable at 30 min and are insignificant even at 1 hr. Results shown in Fig. 11 were calculated under the assumption that the air medium was non-viscous and that geometric sweep-out took place. It is seen that a second q maximum is already evident at 30 min and that transfer of mass to the larger drops accelerates afterward. Indeed, at one hour the 100th largest drop per cubic meter already has a size of 117 μ.

Computations were also carried out with an initial Gaussian spectrum which corresponds to the K-M III spectrum in three respects; i.e., they both have the same liquid water content of 1 gm m^{-1}, the same mean volume radius of 10 μ equivalent to a droplet concentration of 249 cm^{-3}, and approximately the same relative dispersion in r of 0.54. The spectrum evolution is shown in Fig. 12 which should be compared with Fig. 7. These results demonstrate that even with the same relative dispersion the skewed K-M spectrum proceeds with the collection process at a considerable faster rate.

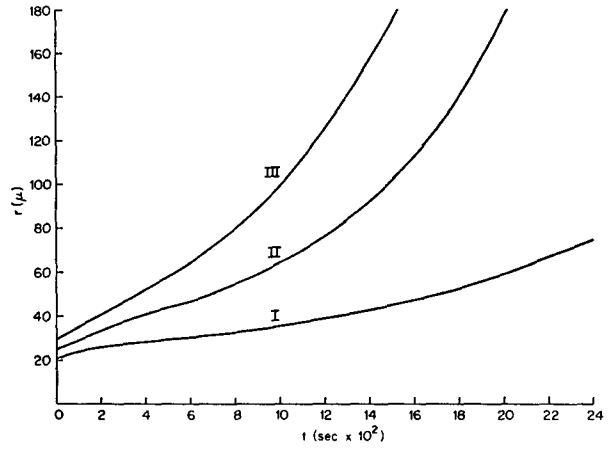

FIG. 9a. Growth of the 100th largest drop per cubic meter for spectra I, II and III.

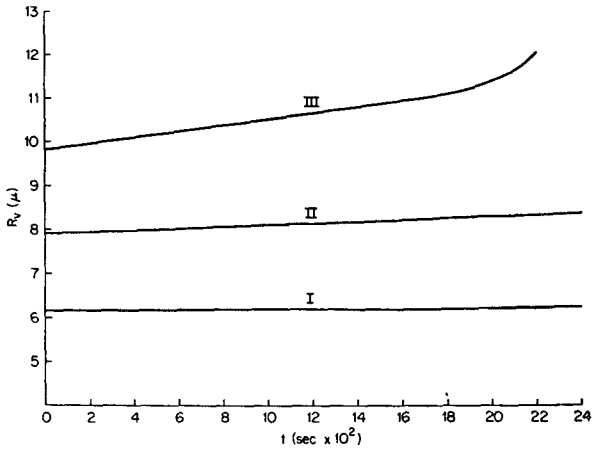

FIG. 9b. Change in mean volume radius R_v for spectra I, II and III.

Berry (1968) proposed that the growth can be divided into three "phases," only in the first of which does the growth depend on the given spectrum. He defined a parameter r_g corresponding to the radius of those drops which are responsible for most of the water mass and gave an expression for the duration T in which r_g would remain less than 40 μ, or equivalently, the duration of the growth would be constrained by the initial spectrum before it could be forgotten. The duration T is a function of the initial droplet concentration, the coefficient of relative dispersion of the initial distribution, and the liquid water content. Using his formulation, we found, for spectrum III, that T was about 15 min; for spectrum II, 26 min; but for a spectrum in which $R_{av}=4.5\,\mu$ and $L=0.3$ gm m^{-3} the predicted time was 172 min, a value which could likely exceed the life expectancy of many such clouds.

4. Comparison of results from the random sampling and kinetic equation approaches

The cloud spectrum can be divided into two non-overlapping parts, one composed of small droplets, the

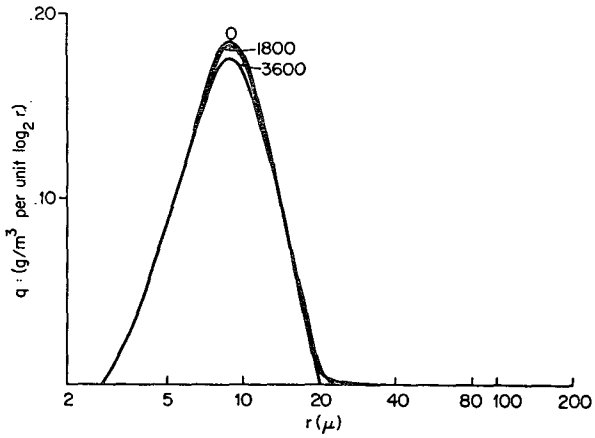

FIG. 10. Evolution of the K-M spectrum due to collection for $L=0.3$ gm m^{-3} and $R_{av}=4.5\,\mu$

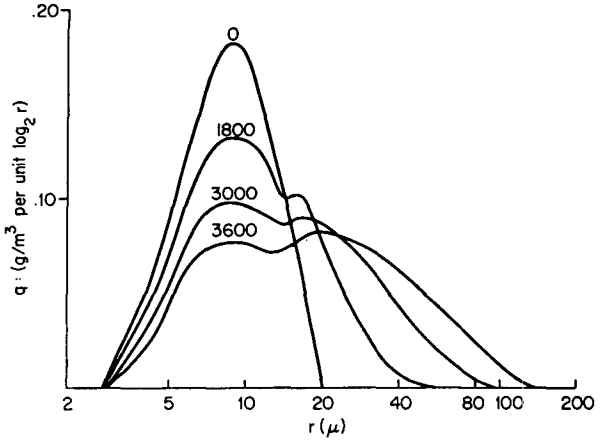

FIG. 11. Evolution of the K-M spectrum due to collection for $L=0.3$ gm m^{-3} and $R_{av}=4.5\,\mu$ in a non-viscous atmosphere with geometric collision efficiency.

other large drops; "small" and "large" are used in a relative sense with respect to a chosen dividing partition. In order to compare our results with those based on random sampling, we assume that the small-droplet side of the spectrum does not change with time. This is felt to be realistic since the collision rates between small droplets are low due to small collision efficiencies and relative velocities. We note, moreover, that the collision rates between large drops themselves are low, again as a result of small collision efficiencies and relative velocities, plus the fact that the large-drop concentration is low. Following Scott (1968), the evolution of the large-drop side of the spectrum will be described by

$$\partial n(v)/\partial t = -n(v)\int_0^{v_1} n_s(u)K(v,u)du + \int_{v_2}^{v} n(v')n_s(v-v')K(v', v-v')dv', \quad (8)$$

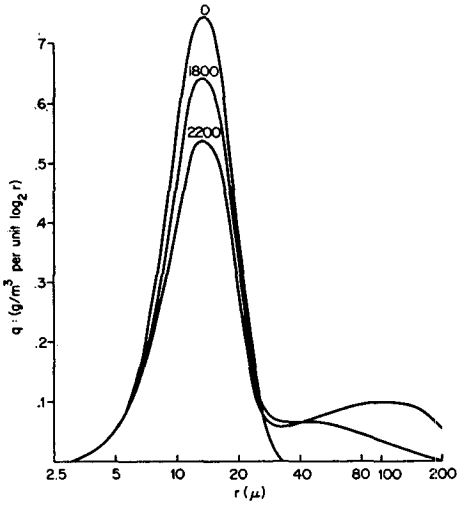

FIG. 12. Evolution of a Gaussian spectrum corresponding to K-M spectrum III.

where v_2 (v_1) is the lower (upper) size limit of the large (small) droplet end of the spectrum with $v_1 \leqslant v_2$; n and n_s denote large and small droplet number densities, respectively; and $n(v) \equiv n(v,t)$, but $n_s(u) = n_s(u,0)$. The main reason for neglecting changes in the small-size end of the spectrum and of disregarding interactions between droplets on the same side of the partition is to have a cloud model compatible with that adopted under the random sampling hypothesis.

Computations were carried out using Eq. (8) under similar initial conditions similar to those of the sampling process; i.e., the small-size part was represented by a K-M III cloud with $R_{av}=7.5\,\mu$, $L=1$ gm m^{-3} and a size range 3 to 29 μ, while the large-size end was initially represented by 32 droplets of 30 μ radius. The numerical procedure used was exactly the same as described previously. As time proceeds, water mass is continuously transferred across the partition toward the large-size side and the size range spreads as the total number of large drops increases. This is in contrast to the random sampling process which also deals with an open system but where the drop number is conserved and the mass increase is distributed among large drops which keep their individual identities. To make a meaningful comparison, the results from these two different approaches were converted into nondimensionalized representations which should be less sensitive to differences in computational procedures.

We define N_{ri} as the total number of droplets which are larger than a given size i, N_t as the total droplet number at time t, and $p_i = v_i N_t / V$, where v_i is the volume of an i-sized droplet and V the initial total volume of large droplets under consideration. A graph of N_{ri}/N_t vs p_i, with p_i extending from a minimum value of 1 upward to cover the whole size range, then represents a dimensionless cumulative distribution of the spectrum at time t. Here we are not referring to the large-droplet spectrum in a unit volume but are considering the *total* number of large droplets in the cloud and their size distribution. In Fig. 13, the smooth curve is the cumulative distribution of the large-droplet spectrum obtained from (8), while the 32 discrete data points have been

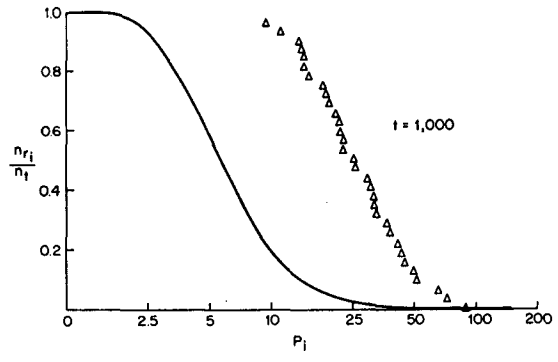

FIG. 13. Comparison of the dimensionless cumulative distributions at $t=1000$ sec between results computed from (9) and those obtained from random sampling.

converted from the random sampling results. Both are for $t=1000$ sec. Substantial deviations between these two results can be found. The overall growth rate of random-sampled droplets is higher while that predicted by the kinetic equation in the form of (8) is more "diffused," with a substantial portion of the mass being contained in relatively small drops and with some rather large drops appearing at extremely low concentrations. Part of the difference in the mass transfer rate from the small-droplet end of the spectrum to the large drops could be due to the fact that the random-sampling method took into account the spatial random distribution of the droplets rather than assuming a homogeneous isotropic cloud.

5. Concluding remarks

A sample of 32 growth histories of droplets initially at a radius of 30μ were generated by independent realizations of the Markov chain growth process in a K-M III cloud environment with droplets randomly positioned in space. At the end of 1000 sec the resulting spread in the sample sizes is such that the sample-mean radius becomes significantly smaller than that predicted by the continuous growth equation applicable to a homogeneous cloud, even though the droplet sample-mean mass is comparable to that forecast by the growth equation. Since the initiation of precipitation depends on the formation and subsequent growth of relatively few large droplets, spatial inhomogeneity in droplet distribution (even when the liquid water content is smooth to a scale of 10 cm) could be a significant factor contributing to the growth process.

Using the continuous growth equation (3), the growth rate of a large droplet in a K-M III cloud was compared to that in a cloud with the same liquid water content, same droplet concentration, but with all droplets having a single size. It was found that at 1000 sec a droplet with an initial radius of 30μ in a monodisperse cloud would attain a mass slightly less than half of that which it would attain in a polydisperse cloud. The monodisperse cloud approximation used in some historical treatments of the growth process would result in an underestimation of the growth rate.

Calculation of cloud spectra evolution with the familiar kinetic equation (5) indicates that the crucial parameter controlling the rate of transfer of water mass toward the large drops is the initial average drop radius R_{av}.

Comparison of the large-droplet growth rate obtained from random sampling at the end of 1000 sec with that predicted by the kineti ecquation (8) for the large-size end of the spectrum shows that the latter approach gave a considerably lower rate of water mass transfer to the large drops. While the resulting disagreement between the dimensionless cumulative distributions of the two spectra (Fig. 13) may be due to some extent to the differences in the numerical methods, a more fundamental factor is felt to be involved. Thus, it is suggested that the spectrum obtained from the kinetic equation should be recognized as an "expected" spectrum. When cloud inhomogeneity is taken into account and a limited number of growth histories of drops are considered for a finite time interval, the resultant growth could deviate substantially from the expected spectrum predicted by the kinetic equation.

Acknowledgments. This research was supported by the Atmospheric Science Section, National Science Foundation, under Grant GA-759.

REFERENCES

Ackerman, B., 1967: The nature of the meteorological fluctuations in clouds. *J. Appl. Meteor.*, **6**, 61–71.

Bartlett, J. T., 1966: The growth of cloud droplets by coalescence. *Quart. J. Roy. Meteor. Soc.*, **92**, 93–104.

Berry, E. X, 1967: Cloud droplet growth by collection. *J. Atmos. Sci.*, **24**, 688–701.

——, 1968: A parameterization of the collection of cloud drops. *Proc. Intern. Conf. Cloud Physics*, Toronto, 111–114.

Bowen, E. G., 1950: The formation of rain by coalescence. *Australian J. Sci. Res.*, **A3**, 193–213.

Davis, M. H., and J. D. Sartor, 1967: Theoretical collision efficiencies for small cloud droplets in Stokes flow. *Nature*, **215**, 1371–1372.

Koo, C. C., 1962: Recent investigations in the theory of the formation of the cloud-drop spectra. *ACTA Meteor. Sinica*, **32**, 267–284.

Kovetz, A., and B. Olund, 1969: The effect of coalescence and condensation on rain formation in a cloud of finite vertical extent. *J. Atmos. Sci.*, **26**, 1060–1065.

Langmuir, I., 1948: The production of rain by a chain reaction in cumulus clouds at temperatures above freezing. *J. Meteor.*, **5**, 175–192.

Nelson, L. D., 1970: A numerical simulation of the effects of water-spray seeding on the warm-rain process. *Preprints of Papers, Second Conf. Weather Modification*, Santa Barbara, Calif., Amer. Meteor. Soc., 18–23.

Scott, W. T., 1968: On the connection between the Telford and kinetic-equation approaches to droplet coalescence theory. *J. Atmos. Sci.*, **25**, 871–873.

Shafrir, U., and M. Neiburger, 1963: Collision efficiencies of two spheres falling in a viscous medium. *J. Geophys. Res.*, **68**, 4141–4148.

Twomey, S., 1966: Computation of rain formation by coalescence. *J. Atmos. Sci.*, **23**, 405–411.

Warshaw, M., 1967: Cloud droplet coalescence: Statistical foundations and a one-dimensional sedimentation model. *J. Atmos. Sci.*, **24**, 278–286.